



Contents lists available at ScienceDirect



Catalysis Today

journal homepage: www.elsevier.com/locate/cattod

Bismuth molybdates prepared by solution combustion synthesis for the partial oxidation of propene

Benjamin Farin^a, Alessandro H.A. Monteverde Videla^b, Stefania Specchia^{b,*}, Eric M. Gaigneaux^{a,**}

^a Institute of Condensed Matter and Nanosciences – MOlecules, Solids and reactiviTy (IMCN/MOST), Université catholique de Louvain, Croix du Sud 2 box L7.05.17, 1348 Louvain-La-Neuve, Belgium

^b Green Energy & Engineering (Gre. En²) Group – Department of Applied Science and Technology, Politecnico di Torino, Corso Duca degli Abruzzi 24, 10129 Torino, Italy

ARTICLE INFO

Article history:

Received 28 October 2014

Received in revised form 16 March 2015

Accepted 18 March 2015

Available online xxx

Keywords:

Solution combustion synthesis

Bismuth molybdates

Propene

Partial oxidation

Acrolein

Selectivity

ABSTRACT

The solution combustion method (SCS) is demonstrated as an easy and fast alternative method allowing the synthesis of mixed oxides with thermally sensitive metals, still keeping a good control on their stoichiometry and phase composition. Bismuth molybdates with different theoretical Bi/Mo atomic ratios, namely α -Bi₂Mo₃O₁₂, β -Bi₂Mo₂O₉, and γ -Bi₂MoO₆ were synthesized by the SCS, fully characterized by XRD, Raman, SEM/EDX, BET and XPS analyses, and tested in the partial oxidation of propene to acrolein. The SCS method allowed obtaining crystalline catalysts with Bi/Mo atomic ratios close to the theoretical values and very good catalytic properties namely high propene conversion (from 13.4 to 23.4%) and acrolein selectivity (from 71.5 to 80.0%) at 425 °C. A high purity of the SCS prepared bismuth molybdates was obtained by means of a subsequent calcination treatment. Such treatment did not alter the high catalytic activity of the catalysts, which slightly increased (from 12.3 to 25.5%), but induced a marked loss of acrolein selectivity (from 66.2 to 48.4%) at 425 °C. This effect is due to a strong increase of the oxidation states of Mo and Bi and reduction of the specific surface area during the calcination.

© 2015 Elsevier B.V. All rights reserved.

1. Introduction

Co-precipitation, high temperature solid-state reactions, spray drying or sol-gel syntheses are the most common methods used to prepare mixed oxide catalysts [1–8]. These routes require severe conditions and long calcination treatments at high temperatures to prepare crystalline materials. This is why the morphology and surface texture of the as-prepared catalysts and thus their resulting catalytic activity are not easily controlled. On this point of view, the solution combustion synthesis (SCS) appears as an elegant alternative protocol. This method is quite simple and presents several advantages. It is based on highly exothermic redox chemical reactions between metallic compounds and non-metallic ones.

The first step of the SCS involves the preparation of an aqueous solution containing suitable metal salts. Nitrates are chosen as metals precursors because of their high solubility in water and the oxidizing potential of NO₃[–] groups. An organic molecule is then

added to the mixture to form complexes with the metal ions and to facilitate the obtaining of a homogeneous solution. The organic molecule works as a fuel as its combustion enables to release a huge amount of heat in a short period of time. Various organic compounds can be used such as urea, glycine, hydrazine or precursors containing a carboxylate anion. The two first compounds are the most convenient ones since they are cheap and readily available commercially. The second step of the SCS process thus consists in heating the final solution until reaching temperatures in the range of 300–450 °C, which brings the solution to ebullition. The resulting mixture then becomes dry and in a matter of minutes ignites what sets off highly exothermic, self-sustaining and fast redox reactions that generate a dry, usually crystalline, fine powder.

The exothermicity of these redox reactions allows reaching temperature peaks that vary from 700 to 1500 °C [9–15]. The very short residence time at high temperature enables synthesizing solid with a minimized occurrence of sintering. Compounds having a relatively high specific surface area can thus be prepared. The rapidity of the method may also allow the formation of metastable phases [9–12]. Finally, a rapid crystallization could favour defects which sometimes enable improving the selectivity of catalysts towards the wished product. The SCS method, in fact, has been favourably used to produce cheaply a huge variety of nanomaterials, such as

* Corresponding author. Tel.: +39 0110904608.

** Corresponding author. Tel.: +32 010473665.

E-mail addresses: stefania.specchia@polito.it (S. Specchia), eric.gaigneaux@uclouvain.be (E.M. Gaigneaux).

catalysts, phosphors, pigments and refractories, for many different applications [16–22].

However, severe conditions as the high-temperatures that are reached during the SCS method appear conflicting with the synthesis of materials made of temperature sensitive metals like molybdenum, rhenium and ruthenium. Among these, MoO₃ indeed sublimates starting from 800 °C [23]. The opportunity to generate temperature sensitive oxides with relatively high specific surface area via the SCS method is then here broached through the synthesis of bismuth molybdates. Three main crystallographic phases of BiMo-mixed oxides are distinguished at atmospheric pressure: Bi₂Mo₃O₁₂ (the α-phase), Bi₂Mo₂O₉ (the β-phase) and Bi₂MoO₆ (the γ-phase) [24–26]. These phases are generally prepared via a solid co-precipitation within an aqueous solution having a Bi/Mo molar atomic ratio equal to 2/3, 1/1 and 2/1, respectively. In the present study, these materials are prepared via the SCS method. A first key question is to evaluate to what extent the SCS method allows preparing bismuth molybdates keeping the control of the stoichiometry and homogeneity of the prepared solids. After their synthesis, the bismuth molybdates are used as catalysts in the propene partial oxidation to acrolein. The second key question is to check whether the simple SCS method is able to produce highly efficient catalysts. This reaction was selected because of the well-known efficiency of bismuth molybdates for the allylic oxidation of olefins. In fact, the reaction's products are important intermediates involved in numerous downstream chemical processes [6,27]. In a world where sustainability and the development of environmentally friendly chemical processes has become a major concern, this work is thus also in line with the efforts trying to improve the valorization of light olefins [28].

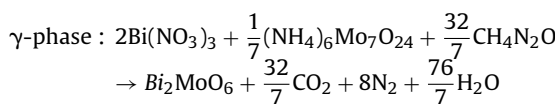
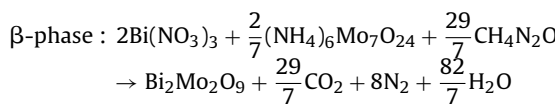
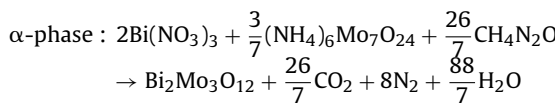
2. Experimental

2.1. Chemicals

Bismuth nitrate pentahydrate (Bi(NO₃)₃·5H₂O, >98% purity), ammonium molybdate tetrahydrate ((NH₄)₆Mo₇O₂₄·4H₂O, >99% purity), and urea (NH₂CONH₂, >99% purity), were purchased from Sigma-Aldrich. Nitric acid (HNO₃, 65 wt.%) was purchased from Merck. All aqueous solutions were prepared using ultrapure water obtained from a Millipore Milli-Q system with a resistivity > 18 MΩ cm⁻¹. Technical grade propene (99.5%), research oxygen and nitrogen (99.999% purity) gases were provided by Praxair and used as received.

2.2. Synthesis of materials

The bismuth molybdates were prepared by the SCS method according to the following stoichiometric reactions:



To prepare 500 mg of each type of catalyst, Bi and Mo precursors, and urea were used in a stoichiometric amount, according to the α-, β-, or γ-phase, and dissolved in ultrapure distilled water. For each catalyst, the obtained solution was thoroughly stirred at

80 °C to ensure the complete dissolution of all reagents. It was then transferred in a ceramic dish and placed into an electric oven set at 430 °C. After water evaporation and a significant increase in the system viscosity, the heat released in the fast reaction allowed the formation of the catalytic powders. The total time necessary to produce the powder was approximately 20 min. Subsequently, after grinding in an agate mortar, half of the prepared powders were calcined in an oven at 425 °C for 4 h in static air, to favour the decomposition of the eventually unreacted nitrate precursors and improve the formation of the desired α, β, or γ crystalline phases. The samples obtained right after the SCS are noted with _F at the end of their label (F for fresh), whereas the calcined ones are noted with _C at the end of their label (C for calcined).

A reference sample (Bi₂Mo₂O₉-Cop) having a Bi/Mo ratio of 1 was also prepared via the co-precipitation method, as described by Carrazan et al. [29]. Bi(NO₃)₃·5H₂O (0.04 mol) was dissolved in a distilled water solution (1 L) heated at 50 °C by using concentrated HNO₃ (0.05 L). (NH₄)₆Mo₇O₂₄·4H₂O (0.006 mol) dissolved in distilled water (0.35 L) was added to the bismuth solution before adjusting the pH at 5 with diluted NH₃ (5 mol L⁻¹). The final solution was stirred for 2 h, aged 24 h and filtered. The recovered solid was dried overnight at 110 °C and calcined at 550 °C, for 4 h, in static air and in a muffle oven. A 5 °C min⁻¹ ramp was used to reach the desired calcination temperature.

2.3. Characterization

X-ray diffraction measurements (XRD) were performed on a Siemens D5000 diffractometer using the K α radiation of Cu ($\lambda = 0.15418$ nm). The 2θ diffractograms were recorded at a rate of 1.2° min⁻¹ between 5 and 75°. The ICDD-JCPDS database was used to identify the detected crystalline phases.

Nitrogen physisorption was performed at -196 °C on a Micromeritics ASAP 2020 instrument. Before the measurement, each sample (about 100 mg) was outgassed overnight at 150 °C in vacuum (7 Pa). The specific surface area was evaluated by the BET method between 0.05 and 0.30 p/p⁰. The pore diameter distribution was evaluated by the Barrett-Joyner-Halenda (BJH) method, calibrated for cylindrical pores according to the improved Kruskal-Jaroniec-Sayari (KJS) method, with the corrected form of the Kelvin equation, from the desorption branches of the isotherms.

Confocal Raman spectroscopy was performed on an InVia Raman microscope (Renishaw) equipped with a diode light (785 nm). The spectra were recorded between 100 and 3500 cm⁻¹ with a 4 cm⁻¹ resolution. 10 scans were recorded and averaged for each sample. Moreover, an acquisition time of 10 s was selected, a laser power was set to 10 mW and the 50× objective was used to focus the apparatus.

Scanning electron microscopy coupled with energy-dispersive X-ray spectroscopy (SEM-EDX FEI-Quanta™ Inspect 200 with EDAX PV 9900 instrument working at 15 kV) was performed to analyze the morphology and evaluate the average chemical composition of the prepared samples. EDX spectra were analyzed with the Genesis Spectrum v. 6.04 (EDAX Inc.) software.

X-ray photoelectron spectroscopy (XPS) was performed using a Physical Electronics PHI 5800 Versa Probe electron spectrometer system with monochromated Al K α X-ray source at 1486.60 eV operated at 25 W, 15 kV, with 100 micron X-rays spot. To reduce any possible charging effects of X-rays, a dual beam charge neutralization method was applied, combining both low energy ions and electrons. The samples were previously outgassed in an ultra-high vacuum chamber at 2.5×10^{-6} Pa for 12 h. Survey scans were recorded from 0 to 1200 eV. The narrow Bi 4f spectra were collected from 148 to 170 eV, the narrow Mo 3d spectra from 218 to 240 eV, and the narrow O 1s spectra from 524 to 536 eV. The samples were analyzed under identical conditions and corrections

referred to C 1s at 284.5 eV, for electrostatic charging. The Multipak 9.0 software was used for obtaining semi-quantitative atomic percentage compositions. The peak position and areas were evaluated using symmetrical Gaussian–Lorentzian equations (in the fraction of 70% and 30%, respectively) with Shirley-type background, and a standard deviation in locating the peaks equal to 0.3 eV.

2.4. Catalytic tests

Bismuth molybdates (0.1 g) were tested in the propene partial oxidation to acrolein at 425 °C and in a 0.04 nL min⁻¹ total flow (C₃H₆/O₂/N₂ = 12.5/25/62.5 vol.%). The catalyst particles (200 μm < D_p ≤ 315 μm) were mixed with 0.4 g of quartz spheres (D_p < 200 μm) previously checked to be inactive and put inside a U-shaped fixed bed quartz reactor with an internal diameter of 4 mm. Thereby, a plug flow was warranted and heat transfer limitations were avoided. A hot-box maintained the gas lines at 100 °C in order to preheat the flow upstream the catalytic reactor. The reaction mixture was analyzed by using an on line Varian GC CP3800. A Hayesep column coupled with a Molecular Sieve column and a TCD detector were used to separate and quantify O₂, N₂, CO and CO₂. The oxygenates (acrolein, propanal, acetone, acetaldehyde and propylene oxide) and propene were detected and quantified by means of an EC-Wax column coupled with a FID detector. Traces of acrylic acid and acetic acid were sometimes detected but not quantified. Carbon balances superior or equal to 90% were calculated from the catalytic results. Here below, the catalytic performances are expressed in terms of propene conversion, product selectivity and acrolein yield.

3. Result

The XRD patterns of the fresh and calcined bismuth molybdates made from the SCS method are shown in Fig. 1 (hereafter named Bi_xMo_yO_z-SCS_F or Bi_xMo_yO_z-SCS_C, respectively). The catalyst

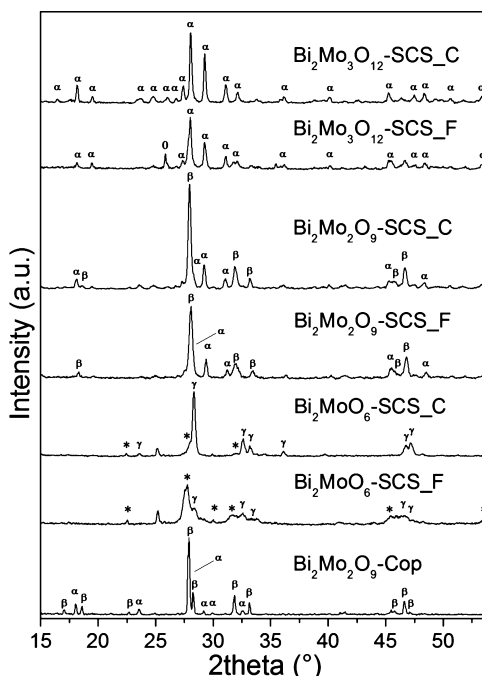


Fig. 1. Diffractograms of fresh and calcined bismuth molybdates prepared by the SCS method. The one of the co-precipitated sample (Bi₂Mo₂O₉-Cop) calcined for 4 h at 550 °C is also shown. α-Bi₂Mo₃O₁₂ (α), β-Bi₂Mo₂O₉ (β), γ-Bi₂MoO₆ (γ) and MoO₂ (0) were identified. The symbol *** refers to a mix of β-Bi₂Mo₃ and β-Bi₂Mo₂O₉ or α-Bi₂Mo₃O₁₂.

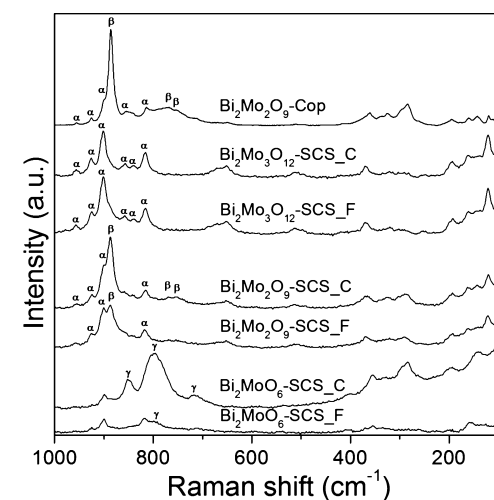


Fig. 2. Raman spectra of fresh and calcined bismuth molybdates prepared by the SCS method. The one of the co-precipitated sample (Bi₂Mo₂O₉-Cop) calcined for 4 h at 550 °C is also shown. α-Bi₂Mo₃O₁₂ (α), β-Bi₂Mo₂O₉ (β), γ-Bi₂MoO₆ (γ) were identified.

prepared by co-precipitation, Bi₂Mo₂O₉-Cop, is also presented. The phases composition of the fresh materials prepared via the SCS method, Bi_xMo_yO_z-SCS_F, is always improved by the 4 h calcination treatment at 425 °C. The materials having a Bi/Mo theoretical ratio of 1/1 (Bi₂Mo₂O₉-Cop, Bi₂Mo₂O₉-SCS_F, and Bi₂Mo₂O₉-SCS_C) display a mix of α- and β-phase regardless the preparation method and the calcination conditions. However, the β-phase systematically remains the dominating phase. The Bi₂Mo₃O₁₂-SCS_F sample presents a mix of α-phase and MoO₂. The latter is easily detected due to the presence of a characteristic sharp peak at $2\theta = 26^\circ$ [30]. A calcination at 425 °C for 4 h of this sample improves the purity of the α-phase as no more MoO₂ is then detected in the Bi₂Mo₃O₁₂-SCS_C. The main reflections of the diffractogram of the Bi₂Mo₆-SCS_F are assigned to a mix of β-Bi₂O₃ and the α- or β-phase. Only small reflections reveal also the minor presence of the desired γ-phase. Nevertheless, the calcination at 425 °C for 4 h favours the crystallization of the γ-phase, which then becomes the dominating crystalline phase in the Bi₂Mo₆-SCS_C catalyst. These observations are confirmed by Raman results whose spectra were analyzed according to data gathered by Li et al. [3], as shown in Fig. 2. The α-Bi₂Mo₃O₁₂ phase is identified by means of six bands at 960, 928, 906, 862, 845 and 818 cm⁻¹, respectively. They correspond to the stretching modes of each tetrahedral molybdate species. The β-Bi₂Mo₂O₉ phase is rather detected through a strong band at 886 cm⁻¹ and two weaker bands at 786 and 754 cm⁻¹ whereas the γ-Bi₂MoO₆ phase displays 3 bands at 852, 796 and 718 cm⁻¹, respectively.

The content of each crystalline phase detected within the samples characterized was calculated by using the following equation [31]:

$$\alpha(\%) = \frac{I_\alpha}{\sum(I_\alpha + I_\beta + I_\gamma + \dots)}$$

where α , β , γ represent a given phase and I the intensity of the strongest XRD reflection. The obtained results are reported in Table 1. The reflections at $2\theta = 27.95$, 27.86 , 28.31 , 27.95 , and 25.81° are the strongest ones of α-Bi₂Mo₃O₁₂, β-Bi₂Mo₂O₉, γ-Bi₂MoO₆, β-Bi₂O₃ and MoO₂, respectively. Since the strongest XRD reflection of the α and β phases are overlapping, the strongest Raman band at 906 and 886 cm⁻¹ were respectively used to determine the composition of samples (Bi/Mo = 1/1) containing both phases.

The Bi/Mo atomic ratio of each catalyst was calculated by EDX and shown in Table 1. Several zones of the samples examined (from

Table 1

Phase composition, specific surface area (BET s.s.a.) and Bi/Mo atomic ratio of BiMo-based materials prepared through the SCS and co-precipitation methods.

Catalysts	Phase composition	Bi/Mo atomic ratio from EDX analysis	BET s.s.a. ($\text{m}^2 \text{g}^{-1}$)
Bi ₂ Mo ₂ O ₉ -Cop	β (79%)+ α (21%)	–	1.0
Bi ₂ MoO ₆ -SCS_F	β or α + β -Bi ₂ O ₃ (81%)+ γ (19%)	1.29–1.37	6.7
Bi ₂ MoO ₆ -SCS_C	γ (84%)+ β and β -Bi ₂ O ₃ (16%)	1.44–1.47	4.3
Bi ₂ Mo ₂ O ₉ -SCS_F	β (52%)+ α (48%)	0.64–0.71	9.3
Bi ₂ Mo ₂ O ₉ -SCS_C	β (63%)+ α (37%)	0.86–0.88	4.0
Bi ₂ Mo ₃ O ₁₂ -SCS_F	α (76%)+MoO ₂ (24%)	0.53–0.58	6.8
Bi ₂ Mo ₃ O ₁₂ -SCS_C	α (100%)	0.65–0.72	2.8

3 to 5 per sample) were screened to check the homogeneity of the samples. These analyses highlight that the Bi/Mo ratios of the samples after the calcination are higher than the ratios for the corresponding fresh samples.

The SEM analysis on the prepared SCS catalysts is shown in Fig. 3, at two different magnification values. Images allow appreciating a spongy-like structure of the fresh catalysts, obtained thanks to the specific technique used to prepare them, because of the very fast reaction combined with the release of the gases from the explosive-like process. BET measurements, listed in Table 1, confirm the relatively high specific surface area of the fresh catalysts, ranging from a maximum value of $9.3 \text{ m}^2 \text{ g}^{-1}$ exhibited by the Bi₂Mo₂O₉-SCS_F to a minimum value of $6.7 \text{ m}^2 \text{ g}^{-1}$ exhibited by the Bi₂MoO₆-SCS_F. However, the calcination of these oxides at 425°C induces a decrease of the specific surface area, ranging from 4.3 (the Bi₂MoO₆-SCS_C) to $2.8 \text{ m}^2 \text{ g}^{-1}$ (Bi₂Mo₃O₁₂-SCS_C), because of possible sintering effects. Despite a higher specific area, the fresh bismuth molybdates prepared by SCS were roughly non porous. The measured total pore volume was indeed quite small and ranged between 0.0040 and $0.0045 \text{ cm}^3 \text{ g}^{-1}$ (coincident with the BJH adsorption cumulative volume of mesopores

with pores within 1.7 and 300 nm), with an average pore size of 2.2 nm.

In agreement with the literature, the bismuth molybdate prepared by co-precipitation has a very low specific surface area ($1 \text{ m}^2 \text{ g}^{-1}$), much lower than all the SCS-calcined catalysts [32]. On the other hand, bismuth molybdates prepared by SCS have higher specific surface area ($6.5\text{--}9 \text{ m}^2 \text{ g}^{-1}$), compared to bismuth molybdates prepared by spray drying ($<2 \text{ m}^2 \text{ g}^{-1}$, [23]).

Table 2 gathers the catalytic performances of the bismuth molybdates in the partial oxidation of propene at 425°C . The materials having a theoretical Bi/Mo ratio of 1/1 are the most active ones (C_{propene} between 23.4 and 25.5%), whereas those having a theoretical Bi/Mo ratio of 2/3 are the less active (C_{propene} around 13%). Intermediate propene conversions (around 18%) are obtained with Bi₂MoO₆-SCS samples. Besides, the activity of the catalysts made from the SCS method is not significantly affected by the calcination treatment. Blank tests performed on all of the prepared catalysts at the same temperature of 425°C showed that there is a few autoxidation of propene into CO₂, equivalent to a propene conversion of maximum 3.5%.

Bi₂Mo₂O₉-Cop rather deeply oxidizes propene as its CO₂ selectivity (66.2%) is superior to its acrolein selectivity (21.3%) (Table 2). At the opposite, the SCS method generates materials being much more selective in acrolein, especially when being fresh (not calcined: $S_{\text{acrolein}} > 71.5\%$). These catalysts, in fact, preferentially produce acrolein to the detriment of CO and CO₂. CO and oxygenates (besides acrolein) remain secondary by-products as their selectivity never exceeds 11.1% and 4.2%, respectively. As in the case of the specific surface area, bismuth molybdates prepared by SCS have higher acrolein selectivity (71.5–80%), compared to bismuth molybdates prepared by spray drying (65–75%, [23]). The calcination of the SCS catalysts at 425°C strongly modifies their selectivity profile. This treatment indeed simultaneously increases the CO₂ production and decreases the acrolein selectivity. This effect is particularly pronounced for the Bi₂Mo₂O₉-SCS_C catalyst whose acrolein selectivity is roughly decreased of about 40% compared to the Bi₂Mo₂O₉-SCS_F catalyst (from 80.0 to 48.4%).

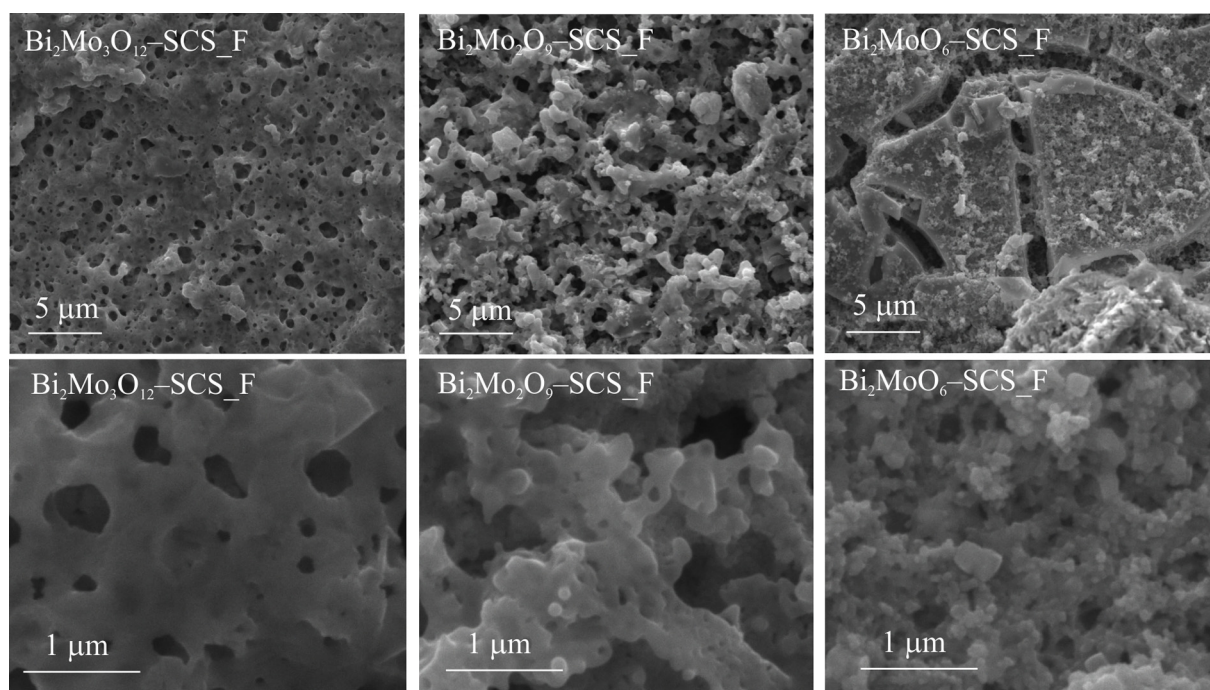


Fig. 3. SEM images at 10,000 \times and 80,000 \times of fresh bismuth molybdates prepared by the SCS method.

Table 2

Propene conversion (C_{propene}), propene reaction rate (RR_{propene}), intrinsic activity (A_{int}), product selectivities (S_{product}), and acrolein yield (Y_{acrolein}) of bismuth molybdates made via the SCS and co-precipitation methods.

Catalyst	C_{propene} (%)	$RR_{\text{propene}}^{\text{b}}$ ($\text{mol m}^{-2} \text{s}^{-1}$)	$A_{\text{int}}^{\text{b}}$ ($\% \text{m}^{-2}$)	S_{acrolein} (%)	S_{CO_2} (%)	S_{CO} (%)	$S_{\text{oxygenates}}^{\text{a}}$ (%)	Y_{acrolein} (%)
$\text{Bi}_2\text{Mo}_2\text{O}_9\text{-Cop}$	20.6	7.659×10^{-6}	206	21.3	63.4	12.1	3.2	3.8
$\text{Bi}_2\text{MoO}_6\text{-SCS.F}$	17.7	9.822×10^{-7}	26.4	77.3	17.3	2.6	2.8	14.0
$\text{Bi}_2\text{MoO}_6\text{-SCS.C}$	18.1	1.565×10^{-6}	42.1	66.2	26.9	4.0	2.9	11.7
$\text{Bi}_2\text{Mo}_2\text{O}_9\text{-SCS.F}$	23.4	9.355×10^{-7}	25.2	80.0	14.8	1.0	4.2	19.0
$\text{Bi}_2\text{Mo}_2\text{O}_9\text{-SCS.C}$	25.5	2.370×10^{-6}	63.7	48.4	36.7	11.1	3.8	11.7
$\text{Bi}_2\text{Mo}_3\text{O}_{12}\text{-SCS.F}$	13.4	7.326×10^{-7}	19.7	71.5	21.4	4.7	2.4	9.3
$\text{Bi}_2\text{Mo}_3\text{O}_{12}\text{-SCS.C}$	12.3	1.633×10^{-6}	43.9	65.3	29.8	2.2	2.7	7.4

^a $S_{\text{oxygenates}}$ regroups the selectivity of acetaldehyde, propanal, propylene oxide and acetone.

^b The reaction rate (RR_{propene}) and the intrinsic activity (A_{int}) refer to the propene reacted or propene conversion, respectively, normalized on the specific surface area and the mass used of the respective catalysts.

At this stage, the acrolein yield of each catalyst can be calculated (Table 2). Compared to $\text{Bi}_2\text{Mo}_2\text{O}_9\text{-Cop}$, the catalysts made from the SCS method are even overall active and much more selective in acrolein. This is why they also display a superior acrolein yield. $\text{Bi}_2\text{Mo}_2\text{O}_9\text{-SCS.F}$ and $\text{Bi}_2\text{MoO}_6\text{-SCS.F}$ are the most efficient catalysts as they display an acrolein yield equal to 17.3 and 14.8%, respectively. For these catalysts, the calcination treatment led to a reduction of the acrolein yield down to 11.7% for both of them. Such a value is anyway much higher compared to the acrolein yield of the $\text{Bi}_2\text{Mo}_2\text{O}_9\text{-Cop}$ catalyst.

On the most critical catalyst, namely the $\text{Bi}_2\text{Mo}_2\text{O}_9\text{-SCS}$, which presented the highest propene conversion and acrolein selectivity at the fresh status, but suffered the highest acrolein selectivity reduction because of the calcination treatment, the XPS analysis was performed. The obtained results are shown in Fig. 4 and in Table 3, as binding energies for Bi 4f, Mo 3d, and O 1s from the decomposition of the high resolution spectra. The Bi/Mo atomic ratio calculated from the XPS shifted from 0.99 for the fresh catalyst to 1.13 for the calcined one, which is the sign of a superficial enrichment of Bi. These values are in agreement with the Bi/Mo atomic ratios calculated by EDX analysis (Table 1). Observing the high resolution spectra of Bi 4f, Mo 3d, and O 1s, their shapes changed markedly from the fresh status to the calcined one. This is the sign of the existence of different chemical species on the surface. Specifically, for Bi 4f spectra, peaks at 156.8 and 162.1 eV on the fresh catalyst disappeared with the calcination. The main top peak of Bi 4f_{7/2} at 159.9 eV can be assigned to Bi^{3+} and, considering

Table 3

XPS analyses: binding energies from the decomposition of the high resolution Bi 4f, Mo 3d, and O 1s spectra for the $\text{Bi}_2\text{Mo}_2\text{O}_9\text{-SCS}$ in the fresh, calcined and used status.

Catalyst	Bi 4f _{7/2}		Mo 3d _{5/2}		O 1s
	Bi^{3+}	Bi^0	Mo^{6+}	Mo^{04+}	
$\text{Bi}_2\text{Mo}_2\text{O}_9\text{-SCS.F}$	159.9	156.8	231.8	228.8	530.3
$\text{Bi}_2\text{Mo}_2\text{O}_9\text{-SCS.C}$	159.8	–	232.2	–	530.3
$\text{Bi}_2\text{Mo}_2\text{O}_9\text{-SCS.U}$	160.1	–	232.6	–	530.7

the standard deviation affecting the measurements, this peak did not shift with the calcination treatment [33,34]. The presence of the peak at 156.8 eV on the fresh spectrum can be assigned to Bi^0 [33,34], which disappeared with calcination. For Mo 3d spectra, the change in the shape indicates the transition from Mo^{6+} to Mo^{04+} (MoO_3) [24,30,34,35], with a small shift in the binding energies to higher values. Considering the O 1s, the spectrum of the fresh catalyst appeared as an asymmetrical peak with a shoulder at lower binding energy. The shoulder reduced drastically in intensity in the calcined catalyst, but the main peak remained centred at the same binding energy. This is the sign that complex oxides are distributed in different amounts [33]. These results are in agreement with the XRD analysis (Table 1 and Fig. 1): the calcined $\text{Bi}_2\text{Mo}_2\text{O}_9\text{-SCS}$ resulted with a higher content of the β -phase respect to the α -phase compared to the fresh $\text{Bi}_2\text{Mo}_2\text{O}_9\text{-SCS}$ catalyst.

Furthermore, on the most interesting catalyst, namely the $\text{Bi}_2\text{Mo}_2\text{O}_9\text{-SCS.F}$, the selective oxidation of propene to acrolein was

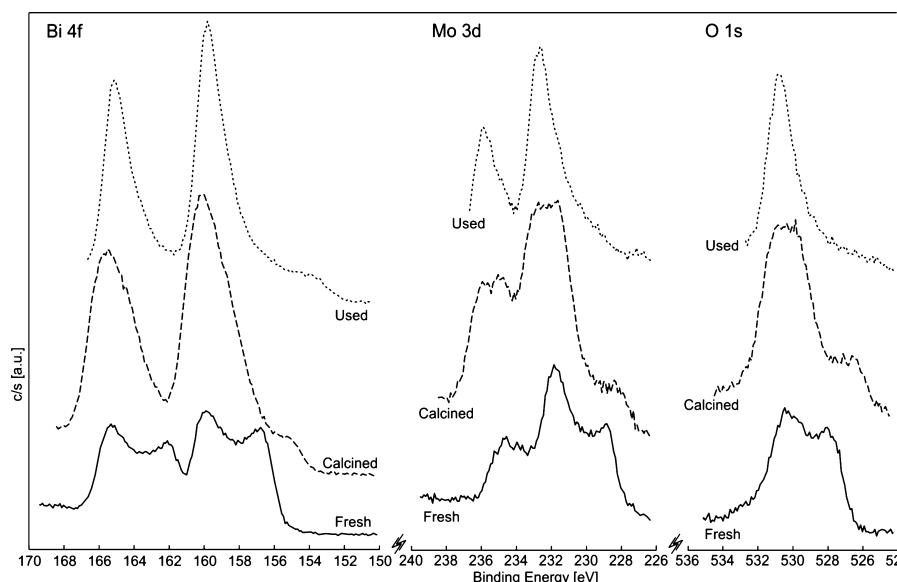


Fig. 4. XPS Bi 4f, Mo 3d, and O 1s high resolution spectra measured on the fresh, calcined, and used $\text{Bi}_2\text{Mo}_2\text{O}_9$ prepared by the SCS method.

conducted at the same conditions previously described for a period of time equal to 20 h, for a first check on the stability. At the end of this time on stream, the propene conversion slightly increased and stabilized at around 25%, and acrolein selectivity dropped down to 47%, with the consequent increase of the carbon dioxide selectivity. The performance results obtained for this catalyst, that is the $\text{Bi}_2\text{Mo}_2\text{O}_9$ -SCS.U where "U" stands for "used" catalyst, are very similar to the results obtained for the calcined catalyst $\text{Bi}_2\text{Mo}_2\text{O}_9$ -SCS.C (Table 2). To document this, BET and XPS measurements were performed on the $\text{Bi}_2\text{Mo}_2\text{O}_9$ -SCS.U catalyst. The BET specific surface area dropped down to $3.6 \text{ m}^2 \text{ g}^{-1}$, namely a value very similar to the BET value of the calcined catalyst $\text{Bi}_2\text{Mo}_2\text{O}_9$ -SCS.C (Table 1). XPS high resolution spectra of the $\text{Bi}_2\text{Mo}_2\text{O}_9$ -SCS.U catalyst are shown in Fig. 4, together with the binding energies of the various high resolution spectra in Table 3. These spectra are very similar to the spectra of the calcined catalyst $\text{Bi}_2\text{Mo}_2\text{O}_9$ -SCS.C. Specifically, the spectrum of the Bi 4f overlapped the spectrum of the calcined catalyst. On the other hand, the spectra of the Mo 3d and O 1s became sharper and more symmetrical, with a slight shift of the binding energies towards higher binding energies (Table 3). The Bi/Mo atomic ratio calculated from the XPS was 1.22, showing an increase compared to value of the calcined catalyst (1.13), which was already increased compared to value of the fresh catalyst (0.99). Thus, the $\text{Bi}_2\text{Mo}_2\text{O}_9$ -SCS.U catalyst, after 20 h of time on stream, appears in a more oxidized state [34], and richer in bismuth.

4. Discussion

The SCS method is suitable to prepare crystalline bismuth molybdates being effective in the selective oxidation of propene into acrolein. According to XRD and Raman results, the desired phase has been successfully obtained (Figs. 1 and 2). However, its purity can be clearly improved by means of a calcination treatment. The increase of the purity corresponds to an increase of the reaction rate expressed as the number of moles of reacted propene normalized on the specific surface area and the mass used of the respective catalysts, as listed in Table 2. These values are better compared to the data calculated for bismuth molybdates synthesized by spray drying (values ranging from 1.8×10^{-7} to 2.8×10^{-7} [23]). According to the SEM pictures (Fig. 3), the SCS method also promotes the rapid crystallization of finely divided materials presenting a higher specific surface area with respect to the co-precipitation method.

The catalytic behaviour of bismuth molybdates can be understood by means of a careful observation of their specific surface area and composition phase. On the one hand, the crystallinity of a bismuth molybdate is necessary to obtain active sites for the conversion of propene into acrolein (i.e., Bi-O-Mo-O) [23]. On the other hand, a high specific surface area is required in order to maximize the number of accessible sites on the catalyst surface. Here, the calcination treatment favours a further crystallization of the samples made by the SCS method to the detriment of their specific surface area (Table 1). This further crystallization then makes the calcined materials more intrinsically active as it is clearly demonstrated in Table 2. The propene conversion drop linked to a specific surface area decrease is then balanced by a propene conversion raise linked to an improvement of the crystallinity. This phenomenon makes the activity of the bismuth molybdates not really sensitive to the calcination treatment. This statement can be strengthened regarding the $\text{Bi}_2\text{Mo}_2\text{O}_9$ -Cop sample which was calcined for 4 h at 550 °C. The very low specific surface area of this sample is balanced by an important crystallinity that maintains its activity at a same level as the $\text{Bi}_2\text{Mo}_2\text{O}_9$ -SCS sample.

While calcination does not affect the activity of bismuth molybdates made from the SCS method, it has got a marked adverse effect

on their acrolein selectivity. This tendency is confirmed regarding the $\text{Bi}_2\text{Mo}_2\text{O}_9$ -Cop sample which presents an acrolein selectivity lower than 20%. A calcination treatment is known to be able to affect both the structure and the catalytic behaviour of catalysts. For example, the sintering of isolated vanadium species in V_2O_5 crystalline particles induces a decrease of the propene selectivity of VO_x/SiO_2 materials in the oxidative dehydrogenation of propane to propene [36]. Here, the calcination causes a further crystallization of the bismuth molybdates and likely favours the formation of sites which overoxidize propene into CO_x . At the opposite, the fresh materials made via the SCS method present an anarchical crystallinity due to the rapid crystallization promoted by the exothermic combustion of an organic fuel. Such materials then rather possess defects and punctual sites being more efficient to selectively oxidize propene to acrolein. The calcination treatment, in fact, clearly cancels the potential of the SCS method to prepare highly acrolein selective materials.

Considering specifically bismuth molybdates, very similar results were obtained by Schuh et al. [2] studying the selective oxidation of propylene to acrolein with catalysts prepared by hydrothermal method. In this case, the catalytic activity of the fresh hydrothermally prepared catalysts was significantly higher than after their calcination (4 h at 550 °C). Furthermore, the obtained acrolein yield, that is proportional to the selectivity, decreased regardless of the phase composition. According to the literature, in fact, calcination time and temperature strongly influence the activity of the bismuth molybdenum catalysts, causing surface enrichment in bismuth after calcination at high temperature or long time exposure [37]. This is exactly what happened to our fresh catalysts after calcination (Tables 1 and 2), and after 20 h of time on stream: with the exposure at high temperature (because of the calcination treatment, or because of the prolonged time on stream in the reactive mixture) the activity remained constant, or slightly increase, whereas the selectivity decreased and the intrinsic activity increased because of the decrease of the specific surface area. Moreover, the surface of the catalyst got enriched in bismuth.

This is in fact demonstrated by the BET and XPS analyses conducted on the fresh, calcined and used $\text{Bi}_2\text{Mo}_2\text{O}_9$ -SCS catalyst. The calcination treatment, in fact, induced a decrease of the specific surface area (Table 1) and a strong variation of the oxidation states of Mo and Bi (Fig. 4). The spectrum of the $\text{Bi}_2\text{Mo}_2\text{O}_9$ -SCS.F, whose acrolein selectivity was the highest, pointed out the presence of Bi_2O_3 and Bi^0 . After the calcination process, metallic Bi disappeared, and simple Bi and Mo oxides appeared. Moreover, a readjustment of superficial oxides gave a Bi rich surface after calcination. Practically the same happened with used catalyst: the only difference between the calcined and the used catalysts lies in the exposure time at high temperature (of course longer for the used catalyst). In agreement with the literature, these results highlight the predisposition of the bismuth molybdates' structure to change. The best catalytic performances were obtained when the surface of the oxide was maintained in a slightly reduced state, as it is the case for the fresh materials prepared by SCS [33,38]. At the opposite, the formation of more stable oxides that results from the calcination treatment, or from the time on stream under the reactive flow, is responsible for a higher intrinsic activity, and higher propene reaction rate, but a lower acrolein selectivity. The resulting effect was thus the decrease of performance in terms of acrolein yield.

Considering the results obtained on the used catalyst $\text{Bi}_2\text{Mo}_2\text{O}_9$ -SCS.U, which confirmed that after 20 h of time on stream the performance was practically the same of the calcined catalyst $\text{Bi}_2\text{Mo}_2\text{O}_9$ -SCS.C (Tables 1–3 and Fig. 4), the calcination treatment performed on the fresh catalyst can be considered as a stabilizing treatment, and the performance of the calcined catalyst can be

considered stable in terms of propene conversion. On the other hand, the acrolein selectivity decreased, whereas the intrinsic activity and the resulting propene reaction rate increased.

5. Conclusion

Bismuth molybdates with different theoretical Bi/Mo atomic ratios, namely α -Bi₂Mo₃O₁₂, β -Bi₂Mo₂O₉, and γ -Bi₂MoO₆ were successfully synthesized by the solution combustion method. SCS thus appears as a suitable technique to prepare highly efficient and selective catalysts, as bismuth molybdates, keeping the control of the stoichiometry and homogeneity of the prepared solids, despite the presence of temperature sensitive metals like molybdenum. SCS catalysts showed very good catalytic results in the partial oxidation of propene to acrolein, particularly in terms of acrolein selectivity. However, after a calcination treatment, which improved their crystallinity, the propene conversion slightly increased but the acrolein selectivity decreased. The calcination treatment, in fact, induced a marked variation of the oxidation states of Mo and Bi, leading to the formation of more stable oxides, with an enrichment of Bi. Efforts must be put to better refining the SCS method, investigating whether the amount of organic fuel used during the SCS synthesis can be optimized, to promote a better crystallization of the material without needing a calcination step. Highly selective materials could then be prepared without affecting their activity level and thus their acrolein yield. SCS also enables to synthesize mixed oxides made of thermally sensitive metals, still keeping a good control on their stoichiometry and phase composition.

Acknowledgments

The authors gratefully acknowledge the 'Fonds pour la formation à la Recherche dans l'Industrie et dans l'Agriculture (FRIA)' of Belgium for financial support and B. Farin's PhD fellowship. Finally, the institute is indebted to the 'Communauté Française de Belgique' for financial support through the ARC programme (08/13-009). The authors thank A.G. Goiri Virto for the assistance in the lab during the SCS of bismuth molybdates. The present research has been conducted under the GDRI Catalyse network "Catalysis for polluting emissions after treatment and production of renewables energies" (2010–2014).

References

- [1] M.T. Le, W.J.M. Van Well, I. Van Driessche, S. Hoste, *Appl. Catal. A: Gen.* 267 (2004) 227–234.

- [2] K. Schuh, W. Kleist, M. Høj, V. Trouillet, P. Beato, A. Degn Jensen, G.R. Patzke, J.-D. Grunwaldt, *Appl. Catal. A: Gen.* 482 (2014) 145–156.
- [3] H.H. Li, K.W. Li, H. Wang, *Mater. Chem. Phys.* 116 (2009) 134–142.
- [4] L.M. Thang, L.H. Bac, I. Van Driessche, S. Hoste, W.J.M. Van Well, *Catal. Today* 131 (2008) 566–571.
- [5] E. Vila, J.E. Iglesias, J. Galy, A. Castro, *Solid State Sci.* 7 (2005) 1369–1376.
- [6] M.D. Wildberger, J.-D. Grunwaldt, M. Maciejewski, T. Mallat, A. Baiker, *Appl. Catal. A: Gen.* 175 (1998) 11–19.
- [7] R.P. Rastogi, A.K. Singh, C.S. Shukla, *J. Solid State Chem.* 42 (1982) 136–148.
- [8] S. Yue, M. Tian, Z. Mao, L. Chen, Y. Zhang, *J. Cryst. Growth* 222 (2001) 747–750.
- [9] S. Specchia, C. Galletti, V. Specchia, *Stud. Surf. Sci. Catal.* 175 (2010) 59–67.
- [10] S. Specchia, E. Finocchio, G. Busca, V. Specchia, *Combustion synthesis*, in: M. Lackner, F. Winter, A.K. Agarwal (Eds.), *Handbook of Combustion*, Wiley-VCH Verlag GmbH & Co. KGaA, Weinheim, 2010, pp. 439–472.
- [11] J.J. Moore, H.J. Feng, *Prog. Mater. Sci.* 39 (1995) 243–273.
- [12] J.J. Moore, H.J. Feng, *Prog. Mater. Sci.* 39 (1995) 275–316.
- [13] K.C. Patil, S.T. Aruna, S. Ekambaran, *Curr. Opin. Solid State Mater. Sci.* 2 (1997) 158–165.
- [14] A. Varma, A.S. Rogachev, A.S. Mukasyan, S. Hwang, *Adv. Chem. Eng.* 24 (1998) 79–226.
- [15] K.C. Patil, S.T. Aruna, T. Mimani, *Curr. Opin. Solid State Mater. Sci.* 6 (2002) 507–512.
- [16] D. Pereira Tarragó, C. de Fraga Malfatti, V. Caldas de Sousa, *Powder Technol.* 269 (2015) 481–487.
- [17] S.I. González-Cortés, F.E. Imbert, *Appl. Catal. A: Gen.* 452 (2013) 117–131.
- [18] G. Liu, J. Li, K. Chen, *Int. J. Refract. Met. Hard Mater.* 39 (2013) 90–102.
- [19] S.T. Aruna, A.S. Mukasyan, *Curr. Opin. Solid State Mater. Sci.* 12 (2008) 44–50.
- [20] S. Ekambaran, K.C. Patil, M. Maaza, *J. Alloys Compd.* 393 (2005) 81–92.
- [21] S. Specchia, A. Civera, G. Saracco, *Chem. Eng. Sci.* 59 (2004) 5091–5100.
- [22] A. Varma, J.-P. Lebrat, *Chem. Eng. Sci.* 47 (1992) 2179–2180.
- [23] M.T. Le, J. Van Craenbroeck, I. Van Driessche, S. Hoste, *Appl. Catal. A: Gen.* 249 (2003) 355–364.
- [24] B. Grzybowska, J. Haber, J. Komorek, *J. Catal.* 25 (1972) 25–32.
- [25] M. Egashira, K. Matsuo, S. Kagawa, T. Seiyama, *J. Catal.* 58 (1979) 409–418.
- [26] R.K. Grasselli, *Top. Catal.* 21 (2002) 79–88.
- [27] M. Massa, A. Andersson, E. Finocchio, G. Busca, F. Lenrick, L.R. Wallenberg, *J. Catal.* 297 (2013) 93–109.
- [28] D.P. Debecker, V. Hulea, P. Hubert Mutin, *Appl. Catal. A: Gen.* 451 (2013) 192–206.
- [29] S.R.G. Carrazán, C. Martín, V. Rives, R. Vidal, *Appl. Catal. A: Gen.* 135 (1996) 95–123.
- [30] J. Wu, H. Yang, Y. Fan, B. Xu, Y. Chen, *J. Fuel Chem. Technol.* 35 (2007) 684–690.
- [31] M.T. Le, W.J.M. Van Well, P. Stoltze, I. Van Driessche, S. Hoste, *Appl. Catal. A: Gen.* 282 (2005) 189–194.
- [32] J. Chul Jung, H. Kim, A.S. Choi, Y.-M. Chung, T.J. Kim, S.J. Lee, S.-H. Oh, I.K. Song, *J. Mol. Catal. A: Chem.* 259 (2006) 166–170.
- [33] K. Uchida, A. Ayame, *Surf. Sci.* 357–358 (1996) 170–175.
- [34] A. Ayame, K. Uchida, M. Iwata, M. Miyamoto, *Appl. Catal. A: Gen.* 227 (2002) 7–17.
- [35] E. Godard, E.M. Gaigneaux, P. Ruiz, B. Delmon, *Catal. Today* 61 (2000) 279–285.
- [36] I. Rossetti, L. Fabbrini, N. Ballarini, C. Oliva, F. Cavani, A. Cericola, B. Bonelli, M. Piumetti, E. Garrone, H. Dyrbeck, E.A. Blekkan, L. Forni, *J. Catal.* 256 (2008) 45–61.
- [37] W.J.M. van Well, M.T. Le, N.C. Schiodt, S. Hoste, P. Stoltze, *J. Mol. Catal. A: Chem.* 256 (2006) 1–8.
- [38] Y. Cui, Y. Xia, J. Zhao, L. Li, T. Fu, N. Xue, L. Peng, X. Guo, W. Ding, *Appl. Catal. A: Gen.* 482 (2014) 179–188.